

# Supernovae-induced accretion and star formation in the inner kiloparsec of a gaseous disk

Pawan Kumar<sup>1</sup> & Jarrett L. Johnson<sup>1,2</sup>

## ABSTRACT

We consider the effects of supernovae (SNe) on accretion and star formation in a massive gaseous disk in a large primeval galaxy. The gaseous disk we envisage, roughly 1 kpc in size with  $\gtrsim 10^8 M_\odot$  of gas, could have formed as a result of galaxy mergers where tidal interactions removed angular momentum from gas at larger radius and thereby concentrated it within the central  $\sim 1$  kpc region. We find that SNe lead to accretion in the disk at a rate of roughly  $0.1\text{--}1 M_\odot \text{ yr}^{-1}$  and induce star formation at a rate of  $\sim 10\text{--}100 M_\odot$  per year which contributes to the formation of a bulge; a part of the stellar velocity dispersion is due to SNa shell speed from which stars are formed and a part due to the repeated action of stochastic gravitational field of SNe remnant network on stars. The rate of SNa in the inner kpc is shown to be self regulating, and it cycles through phases of low and high activity. The supernova-assisted accretion transports gas from about one kpc to within a few pc of the center. If this accretion were to continue down to the central black hole then the resulting ratio of BH mass to the stellar mass in the bulge would be of order  $\sim 10^{-2}\text{--}10^{-3}$ , in line with the observed Magorrian relation.

*Subject headings:* accretion: theory, method: analytical – supernovae – stars: formation – galaxies: bulges

## 1. Introduction

The CO observations of ultra-luminous infra-red galaxies (ULIGals) find the gas mass in the inner regions of the galaxy to be about  $5 \times 10^9 M_\odot$ , and the average particle density to be of order  $10^3 \text{ cm}^{-3}$  and the kinetic temperature of molecular gas  $\sim 50\text{--}100$  K (e.g. Downes & Solomon, 1998; see Sanders & Mirabel, 1996, for a review). The gas in the central  $\sim$ kpc region of the galaxy is likely to have come from distances of the order of 10 kpc when it lost some of its angular momentum due to gravitational tidal torques (Barnes & Hernquist, 1992, and references therein; see Barnes, 2002, for a more recent numerical simulation).

---

<sup>1</sup>Astronomy Department, University of Texas at Austin, Austin, TX 78712

<sup>2</sup>Theoretical Modeling of Cosmic Structures Group, Max-Planck-Institut für extraterrestrische Physik, Giessenbachstraße, 85748 Garching, Germany

The inner kiloparsec region of most young massive galaxies is likely composed of a gaseous disk with a mass of several hundred million solar masses, ULIGal being at the extreme end of the mass distribution. This gaseous disk is expected to host star formation at a large rate. Some of these stars will explode and give rise to shock waves in the gaseous disk which will spawn both more star formation and accretion of gas toward the center of the galaxy. We consider these processes analytically in some detail in this paper, paying special attention to the effect they might have on the evolution of the central parts of the galaxy and on the growth of a central black hole.

There exists a large body of work on the subject of galaxy mergers, star formation and black hole growth e.g. Sanders et al. (1988), Kauffmann & Haehnelt (2000), Kawakatu & Umemura (2002), Granato et al. (2004), Croton et al. (2006), Kauffmann & Heckman (2009), Chen et al. (2009), (pl. see Kormendy & Kennicutt, 2004, for a review), and sophisticated numerical simulations e.g. Barnes & Hernquist (1991, 1996), Mihos & Hernquist (1996), Di Matteo et al. (2005), Springel et al. (2005), Hopkins et al. (2005), Hopkins & Hernquist (2008). What is different in the present work is that we try to capture some of the basic properties of this complex system using analytic results for supernova (SNa) remnant evolution and other simple physical scalings which are hard to capture in numerical simulations due to the large ratio of galaxy size and SNa shell radius.

The physical system we consider is described in §2 along with the effect SNe have on accretion. Bulge formation as a product of SN-induced star formation in the gaseous disk is discussed in §3. The main conclusions and uncertainties of this study can be found in §4.

## 2. Supernovae-induced accretion in a gas disk

Numerical simulations of gaseous disks (e.g. Wada & Norman, 2001) find the medium to be multi-phase and highly filamentary as a result of star formation and stellar explosion. For the analytical calculations in this work, where our primary interest is in average disk properties, we consider a simplified disk structure that ignores its filamentary density structure; accordingly, the gas distribution is taken to be a smooth function of distance from the center. Many of the results reported in this work, as we shall see, have a weak dependence of the interstellar medium (ISM) density and therefore the error introduced by the assumption of smooth density field in the disk should not be large.

We consider a disk, roughly 1 kpc in radius, consisting of  $\gtrsim 10^8 M_{\odot}$  in gas that came from larger radius ( $\sim 10$ s kpc) due to e.g., tidal interaction with another galaxy. The mean gas density in the disk at 1 kpc is  $\sim 10^3 \text{ cm}^{-3}$ . Stars form and die in the disk at a certain rate; we take the SNa rate in the disk to be  $df_{sn}(r)/dA$  per unit area per year. The interaction between the remnant of a supernova with the gaseous disk carves out a cavity in the disk. The gas swept up by a supernova is compressed into a thin shell during the snowplow phase, which starts when the thermal cooling time scale of the shocked gas is less than the age of the remnant. This means

that a certain amount of gas is pushed closer to the galactic center by the supernova shock wave and, of course, a certain amount is pushed outward. However, unless gas pushed inwards by the supernova shock loses angular momentum it will be pushed back out to a larger radius when the shock weakens. We shall estimate later in this section the loss of angular momentum for gas pushed closer to the galactic center by the SNa, in order to determine if it is sufficient to keep the swept up gas at a smaller radius. But first, we estimate the amount of gas swept up and pushed to smaller radius by a supernova.

Let us consider a supernova going off in the disk at radius  $r$ . The number density of particles in the disk at this radius is  $n(r)$ , the vertical scale height is  $H(r)$ , and the mean rotation speed of gas on its circular orbit is  $V_{orb}(r)$ . During the adiabatic expansion of the SNa shell – the Sedov-Taylor phase – the radius, speed and temperature of the shock front are given by

$$R_s(t) = 3.1t_4^{2/5}n_3^{-1/5}E_{51}^{1/5} \text{ pc}, \quad (1)$$

$$V_s(t) = 123t_4^{-3/5}n_3^{-1/5}E_{51}^{1/5} \text{ km s}^{-1}, \quad (2)$$

$$T(t) = 2.1 \times 10^5 t_4^{-6/5} n_3^{-2/5} E_{51}^{2/5} \text{ K}, \quad (3)$$

where  $t_4 = t/10^4 \text{ yrs}$ ,  $E_{51} = E/10^{51} \text{ erg}$ , and  $n_3 = n/10^3 \text{ cm}^{-3}$  is the particle number density of gas in the disk at radius  $r$ . The Sedov-Taylor phase ends when the radiative cooling time  $t_{cool} = 0.67kT/(n\Lambda)$  is equal to the dynamical time;  $\Lambda \approx 10^{-16} T^{-1} \text{ ergs cm}^3 \text{ s}^{-1}$  (Blondin et al. 1998). The radiative phase begins at time

$$t_{snow} \approx 723n_3^{-9/17}E_{51}^{4/17} \text{ yrs}. \quad (4)$$

Subsequently, during the snowplow phase ( $t > t_{snow}$ ), the evolution is described by (cf. Chevalier, 1974; eq. 26)

$$R_s(t) \approx 0.8(t/t_{snow})^{0.31}n_3^{-7/17}E_{51}^{5/17} \text{ pc}, \quad (5)$$

$$V_s(t) \approx 595(t/t_{snow})^{-0.69}n_3^{2/17}E_{51}^{1/17} \text{ km s}^{-1}, \quad (6)$$

$$M_s(t) \approx 133(t/t_{snow})^{0.93}n_3^{-4/17}E_{51}^{15/17} M_\odot, \quad (7)$$

where  $M_s$  is the mass of gas swept up by the SNa remnant. These equations are valid only as long as the shell radius is less than the vertical scale-height  $H$ :

$$H = \frac{2^{1/2}(C_s^2 + V_t^2)^{1/2}}{\Omega} = \frac{2^{1/2}r(C_s^2 + V_t^2)^{1/2}}{V_{orb}} \sim (500 \text{ pc}) r_3^{3/2} \left( \frac{V_t}{10 \text{ km s}^{-1}} \right) \left( \frac{M(r)}{10^8 M_\odot} \right)^{-1/2} \quad (8)$$

where  $r_3 = r/10^3 \text{ pc}$ ,  $C_s \sim 1 \text{ km s}^{-1}$  is the sound speed,  $V_t$  is the RMS turbulence velocity in the gaseous disk (produced by SNa explosions and winds from early type stars), and  $M(r)$  is the total mass enclosed within radius  $r$ .

The Toomre  $Q$  parameter for the gravitational instability of the gaseous disk is:

$$Q = \frac{2(C_s^2 + V_t^2)^{1/2}\Omega}{\pi G \Sigma} \sim 1 V_{t,6} M_8^{-1/2} r_3^{1/2}, \quad (9)$$

where  $\Sigma$  is the mass density per unit area,  $V_{t,6} \equiv V_t/10^6 \text{ cm s}^{-1}$ , and  $M_8 \equiv M(r)/10^8 M_\odot$ . We see from the above equation that the disk is gravitationally unstable, and will support an on-going star formation activity.

Ignoring density gradients in the disk ( $R_s \ll r$  &  $R_s < H$ ), the expansion of a SNa shell is nearly spherically symmetric until the Coriolis or centrifugal force per unit mass becomes of order the deceleration of SNa remnant. This occurs when  $V_s \Omega_{orb} \approx dV_s/dt$ , or  $t \approx 0.69/\Omega_{orb}$ , and defines a characteristic time when the shell is no longer spherical.

$$t_{shear} \approx 7 \times 10^6 r_3 V_{orb,2}^{-1} \text{ yrs} \quad (10)$$

where  $V_{orb,2} = V_{orb} / 100 \text{ km s}^{-1}$ . In fact, at this time the magnitude of the shear velocity across the shell –  $R_s d\Omega_{orb}/d \ln r$  – is of order the speed of the SNa remnant. The SNa shell is thus dispersed by the shear flow in the disk and mixed with the ambient ISM on this time scale. The radius, velocity and mass of the remnant at this time is

$$R_s(t_{shear}) \sim 14 n_3^{-0.25} E_{51}^{0.22} r_3^{0.31} V_{orb,2}^{-0.31} \text{ pc}, \quad (11)$$

$$V_s(t_{shear}) \sim 1.1 n_3^{-0.25} E_{51}^{0.22} V_{orb,2}^{0.69} r_3^{-0.69} \text{ km s}^{-1}, \quad (12)$$

$$M_s(t_{shear}) \sim 7 \times 10^5 r_3^{0.93} V_{orb,2}^{-0.93} n_3^{0.25} E_{51}^{0.66} M_\odot. \quad (13)$$

Note that  $R_s(t_{shear}) \lesssim H$ , and therefore the SNa shell is confined within the disk unless  $r \lesssim 10 \text{ pc}$ . Since the shell velocity is small compared with the orbital speed when  $R_s \sim H \text{ pc}$ , the swept up gas in the disk cannot escape the galactic potential.

During the snowplow phase the swept-up gas is compressed into a thin shell, forming a hollow sphere. Therefore, half of the swept up ISM gas, of mass  $M_s/2$ , is pushed closer to the center of the galaxy by a distance  $\sim R_s/2$ . For an ensemble of SNe going off in the disk the net amount of gas that is accreted at  $r$  depends on the SNe rate as a function of distance from the galactic center ( $r$ ) and is given by

$$\dot{M}_{acc} \sim R_s \frac{d}{dr} \left( \frac{M_s(r)}{2} [2\pi r R_s] \frac{df_{sn}}{dA} \right) \sim M_s (R_s/r)^2 f_{sn}(r) \quad (14)$$

where  $f_{sn}(r)$  is the cumulative SNa rate within the radius  $r$ . We assumed that  $(M_s R_s f_{sn}/r)$  is an increasing function of  $r$  in deriving the second part of the above equation; otherwise, SNe would lead to a net outflow of gas in the disk to larger distances. Since  $M_s R_s \propto n^{0.01}$  during the snowplow phase (combine eqs. 5 & 7, & substituting for  $t_{snow}$  from eq. 4) as long as  $f_{sn}(r)$  increases with distance faster than  $r^1$  there is a net mass accretion even when SNa remnants are spherically symmetric. For a Mestel disk the mass enclosed inside radius  $r$  increases linearly with  $r$ , and in that case there is no net accretion – for spherical SNe – if the rate of stellar explosions is linearly proportional to gas mass. We shall see below that the condition on  $f_{sn}(r)$  is relaxed when we consider the distortion of SNe remnants by Coriolis and centrifugal forces. Equation (14) for accretion rate is also modified when SNe shells undergo collision before  $t_{shear}$ ; this is discussed

below. However, in any case we need to make sure that gas pushed inward by a SNa loses specific angular momentum; otherwise, it would be pushed back out when the shock becomes sufficiently weak.

It should be noted that half of a SNa shell has negative angular momentum (as seen by an observer at the center of the explosion comoving with the disk), and the other half, with prograde velocity field, has positive angular momentum. The magnitude of the total positive/negative angular momentum grows during the adiabatic expansion as  $|L_{\pm}| \approx M_s V_s r / 2 \propto 1/V_s$  (the second part of this relation follows from energy conservation during the adiabatic expansion phase). However, the angular momentum does not increase much during the snowplow phase when  $M_s V_s$  is approximately constant. The magnitude of the negative angular momentum carried inward by the lower half of a SNa shell ( $|L_-|$ ) is quite large and that can lead – as we shall see shortly – to an accretion rate in a gas rich disk (like ULIGal) of order a few solar masses per year.

It can be shown that, for a freely expanding shell, particles on half of the shell with negative angular momentum – that have retrograde velocity as seen by a comoving observer at the center of explosion – will on average descend a distance of  $\Delta r = (8V_{orb}/\pi V_s - 1)R_s^2/4r$  in the radial direction (as a result of Coriolis and centrifugal forces in the comoving frame), as long as  $V_s \gtrsim R_s |d\Omega_{orb}/d \ln r|$ . Particles on the other half of the shell with positive angular momentum, or prograde velocity, will move outward the same distance. Thus, the shell is continuously distorted with time as a result of tidal stretching and Coriolis force.

Part of the lower half of the shell (lying closer to the galactic center) with transverse velocity component in the direction of the orbital velocity has a positive angular momentum with respect to the center of explosion, and the part with transverse velocity opposite to the orbital motion has negative specific angular momentum. The net amount of negative angular momentum carried by the distorted lower half of the shell, during the snowplow phase, as seen by an observer comoving with the center of explosion, is

$$\delta L \approx \Delta r (L_- / R_s) \approx M_s R_s V_{orb} / \pi. \quad (15)$$

When the lower half of the shell is mixed – due to shear stretching or collision with other shells – the net mean specific angular momentum of the mixed fluid is smaller by  $\sim 2R_s V_{orb} / \pi$  than a particle at the center of the explosion orbiting the galaxy. This is a sufficient amount of negative angular momentum to keep the mixed lower half of shell moving on a circular orbit at a smaller radius of  $(r - R_s/2)$ . Thus, the constraint discussed earlier on  $f_{sn}$  for inward mass accretion is relaxed because there is a net outward transport of positive angular momentum associated with each SNa shell.

The rate of angular momentum transported by an ensemble of SNe in the disk is

$$\dot{L} \sim \delta L (2\pi r R_s) \frac{df_{sn}}{dA} \sim \frac{2M_s}{\pi} R_s V_{orb} (R_s/r) f_{sn}, \quad (16)$$

and the accretion rate resulting from this outward angular momentum transport is

$$\dot{M}_{acc} \approx \frac{\dot{L}}{rV_{orb}} \approx \frac{2M_s f_{sn}}{\pi} \left( \frac{R_s}{r} \right)^2, \quad (17)$$

which is similar in magnitude to that given by equation (14), i.e. SNe transport mass inward for a larger class of functions for  $f_{sn}(r)$  than suggested by the discussion following equation (14).

The accretion rate depends on the shell radius ( $R_s$ ) at the time when SNe shells collide with each other or when the shell is dispersed and mixed due to shear flow in the disk. We consider both of these cases below.

Given a supernova rate of  $f_{sn}$  per year within radius  $r$  of the disk, the mean separation between SNe that occurred within time  $t$  is

$$d_{sn} \approx 1.8 \frac{r}{1\text{kpc}} \left( \frac{t}{1\text{yr}} \right)^{-1/2} f_{sn}^{-1/2} \text{ kpc}. \quad (18)$$

SNe shells collide when their size is of order the mean separation i.e.  $R_s(t) \approx d_{sn}$ . The mean collision time,  $t_{coll}$ , is estimated using equation (5), and is given by

$$t_{coll} \approx 1.7 \times 10^5 n_3^{0.31} f_{sn}^{-0.62} E_{51}^{-0.27} r_3^{1.23} \text{ yrs}. \quad (19)$$

The ratio of the collision time and the time it takes for a SNa shell to be dispersed due to shear velocity in the disk is

$$\frac{t_{shear}}{t_{coll}} \approx 40 n_3^{-0.31} f_{sn}^{0.62} r_3^{-0.23} V_{orb,2}^{-1} E_{51}^{0.27}. \quad (20)$$

The accretion rate when  $t_{shear}/t_{coll} \lesssim 1$  is given by (using eqs. 11, 13 & 17)

$$\dot{M}_{acc} \sim M_s(t_{shear}) f_{sn} \left[ \frac{R_s(t_{shear})}{r} \right]^2 \sim 80 f_{sn} n_3^{-0.25} r_3^{-0.45} V_{orb,2}^{-1.55} E_{51}^{1.1} M_\odot \text{ yr}^{-1}. \quad (21)$$

The condition for a remnant not to collide with others before  $t_{shear}$  places a limit on the supernova rate of

$$f_{sn} \lesssim 3 \times 10^{-3} n_3^{1/2} V_{orb,2}^{1.6} r_3^{0.37} E_{51}^{-0.44} \text{ yr}^{-1} \equiv f_{sn}^{coll}. \quad (22)$$

The second part of eq. (21) is valid only when the SNa rate is less than the rate given in eq. (22); the accretion rate corresponding to this limiting SNa rate is

$$\dot{M}_{acc} \sim 0.3 n_3^{0.25} E_{51}^{0.66} r_3^{-0.08} V_{orb,2}^{0.05} M_\odot \text{ yr}^{-1}, \quad (23)$$

The accretion rate has a very weak dependence on  $f_{sn}$  when the SNa rate is larger than the rate given in equation (22), i.e. when SNe shells collide before  $t_{shear}$ . The reason is that the SNa shell radius at the time of shell collision ( $t_{coll} \propto f_{sn}^{-0.62}$ ) is  $R_s \propto f_{sn}^{-0.19}$  and the shell mass is  $M_s \propto R_s^3 \propto f_{sn}^{-0.57}$ ; therefore, the accretion rate  $\dot{M}_{acc} \sim M_s (R_s/r)^2 f_{sn} \propto f_{sn}^{0.05}$ . For the case of  $t_{shear}/t_{coll} > 1$ , the accretion rate is given by:

$$\dot{M}_{acc} \approx 0.3 n_3^{0.25} f_{sn}^{0.05} E_{51}^{0.7} r_3^{-0.14} M_\odot \text{ yr}^{-1}. \quad (24)$$

For  $\dot{M}_{acc}$  to be independent of  $r$  the density should scale as  $f_{sn}(r)^{-0.2}r^{0.5}$ . However, for a non-equilibrium situation in the early phases of galaxy formation and frequent mergers this equilibrium density scaling is not applicable. When a large quantity of gas is deposited within a few kpc following a merger event or a tidal encounter, the high rate of star formation and SNe at  $r \sim 1$  kpc would cause a rapid rate of accretion of gas to smaller radii,  $\dot{M}_{acc} \sim M_s(t_{shear})f_{sn} \sim 10^7 M_\odot f_{sn} \text{ yr}^{-1}$  after a lag of  $\sim 10^7$  yrs, which will continue until star formation and SNa explosions at smaller radii start to inhibit this large accretion rate; The subsequent accretion rate would settle down to the value given by equation (24).

Note that the cumulative effect of SNe is to create a random velocity field in the disk, but that does not automatically ensure accretion. We must have an outward angular momentum transport in order for accretion to proceed. An interesting example is that of convective instability in a disk; Ryu & Goodman (1992) have shown that disk-convection transports angular momentum inward, and therefore the turbulent velocity field associated with it does not lead to any accretion. Similarly, the random velocity field in a disk is large when the SNa rate is high and yet because shells collide before they are significantly deformed the outward transport of angular momentum increases very weakly with  $f_{sn}$  (eq. 24). The accretion rate in terms of an effective  $\alpha$ -viscosity,  $\nu \equiv \alpha R_s(t_{coll})V_s(t_{coll})$ , in the limit that  $f_{sn} > f_{sn}^{coll}$  is given by

$$\dot{M}_{acc} \sim 2\pi m_p n H \nu \sim 1.2\alpha (H/0.1r) n_3^{0.39} f_{sn}^{0.24} E_{51}^{0.54} r_3^{0.53} M_\odot \text{ yr}^{-1}. \quad (25)$$

Comparing this with equation (24) we see that  $\alpha \sim 1$  for  $f_{sn} \sim f_{sn}^{coll}$  (given by eq. 22), and  $\alpha$  is smaller for a larger SNa rate, although the effective  $\alpha$  is dependent on  $r$ .

If SNe remnants punch through the disk in the vertical direction, but are still confined by the galactic potential, then some fraction of gas leaving the disk will eventually fall back onto the disk at a smaller radius and contribute to the net accretion rate. A SNa is confined to the galaxy provided that

$$R_s(\min\{t_{coll}, t_{shear}\}) < H \quad \text{or} \quad V_s(R_s = H) < V_{orb}. \quad (26)$$

If many SNe shells collide and coalesce before they are dispersed they would form super-shells and if their velocity is sufficiently high they can escape the galactic potential. Otherwise, these super-shells would also contribute to transporting gas to smaller radius.

### 3. Star and bulge formation and growth of a central black hole

The possibility of SNa-induced star formation has been discussed in numerous contexts, from the early universe to the present day Milky Way (e.g. Woodward 1976; Bedogni & Woodward 1990; Yamada & Nishi 1998; Mackey et al. 2003; Bratsolis et al. 2004; Joung & Mac Low 2006; Johnson & Bromm 2006; Sakuma & Susa 2009; Leão et al. 2009; Nagakura et al. 2009). Here we consider how this process may compete with the fueling of black holes and contribute to the formation of galactic bulges.

For a Miller-Scalo initial-mass function (IMF) for stars (Scalo, 1986):

$$\frac{dN}{dM} = 4.5N_* \times \begin{cases} 1.9(M/0.01M_\odot)^{-\alpha_1} & 0.01M_\odot < M \leq 0.08M_\odot \\ (M/0.08M_\odot)^{-\alpha_2} & 0.08M_\odot < M \leq 0.5M_\odot \\ 6.25^{-\alpha_2}(M/0.5M_\odot)^{-\alpha_3} & M > 0.5M_\odot, \end{cases} \quad (27)$$

with  $\alpha_1 = 0.3$ ,  $\alpha_2 = 1.8 \pm 0.5$ ,  $\alpha_3 = 2.3 \pm 0.7$  (the parameters are taken from Kroupa, 2001), and  $N_* = \int dM dN/dM$ . The mass fraction in high mass stars ( $M_* \gtrsim 8M_\odot$ ), capable of SNa explosion, to the total star mass is about 0.3, and the fraction by number is about  $4 \times 10^{-3}$ . Thus the expected SNa rate is  $0.3 \text{ yr}^{-1}$  for the Miller-Scalo IMF and a star formation rate (SFR) of  $10 M_\odot \text{ yr}^{-1}$ , which is of the order observed in ULIGals and needed for forming galactic bulges in  $L_*$  galaxies.

Indeed, this is consistent with the following simple estimate of the star formation rate in the gaseous disk:

$$SFR \sim f_* M_{\text{disk}}/t_{\text{ff}}, \quad (28)$$

where  $M_{\text{disk}}$  is the disk gas mass,  $t_{\text{ff}}$  is the free-fall time, and  $f_*$  is the efficiency with which gas is turned into stars on a free-fall time, taken to be of the order of  $f_* \sim 0.01$  (e.g. Krumholz & Tan 2007). Then, for a disk of  $10^8 - 10^9 M_\odot$ , the SFR is about 1-10  $M_\odot$  per year, assuming a density of  $10^3 \text{ cm}^{-3}$ .

If a similar fraction ( $\sim 1\%$ ) of gas in SNe shells is turned into stars (before shells collide) then the resulting star formation rate would be  $\sim 140M_\odot n_3^{0.54} E_{51}^{0.4} r_3^{1.1} f_{sn}^{0.4} \text{ yr}^{-1}$ , and that would result in a SNa rate of  $\sim 5n_3^{0.54} E_{51}^{0.4} r_3^{1.1} f_{sn}^{0.4} \text{ yr}^{-1}$  if the IMF for these “daughter” stars were given by equation (27). However, we show below that formation of massive stars – those capable of SNa explosion – is suppressed in SNe remnants when  $f_{sn} \gtrsim 0.5$ .

Star formation in a SNa shell is suppressed on large length scales due to the transverse relative velocity gradient in the remnant. We calculate this length scale as well as the Jean’s length, and estimate the rate of star formation in SNe-remnants.

The velocity field in a SNa remnant seen by a comoving observer in her neighborhood is:  $\delta\vec{V}_s \sim (V_s/R_s)\delta\vec{r}$ ; where  $\delta\vec{r}$  is the position vector, tangential to the shock front, pointing from the comoving observer to a point in her neighborhood. For a gas clump to be able to collapse, the differential velocity across the clump,  $|\delta\vec{V}_s|$ , should be smaller than the gravitational escape speed, i.e. for a clump of size  $\ell$ ,  $|\delta\vec{V}_s| \sim V_s(\ell/R_s) < [GM_s(\ell/R_s)^2/4\ell]^{1/2}$  or

$$\ell \lesssim \frac{GM_s}{4V_s^2}, \quad M_\ell \sim M_s(\ell/2R_s)^2 \sim \frac{G^2 M_s^3}{64V_s^4 R_s^2} \quad (29)$$

Using equations (5)–(7) we find

$$M_\ell \sim 9 \times 10^{-12} \left[ \frac{t}{t_{\text{snow}}} \right]^{4.9} n_3^{-\frac{6}{17}} E_{51}^{\frac{31}{17}} M_\odot, \quad (30)$$



We see from equation (6) that at  $t/t_{snow} \approx 137n_3^{0.17}E_{51}^{0.09}$  the shell speed is  $V_s = 20 \text{ km s}^{-1}$ , and at that time  $M_\ell \sim 0.2n_3^{0.48}E_{51}^{2.2} M_\odot$ ; the maximum star mass scales as  $V_s^{-7.1}$ .

Star formation is disrupted when shells collide<sup>1</sup>. The average speed of SNe shells when they collide, at time  $t_{coll}$ , is  $V_s \sim 14 \text{ km s}^{-1} f_{sn}^{0.4} r_3^{-0.8} n_3^{-0.5} E_{53}^{0.4}$  (obtained from equations 6 & 19). For a small SNa rate,  $f_{sn} < 0.5 \text{ yr}^{-1}$ ,  $V_s$  can drop down to a value where massive stars capable of SNa explosion can form before SNe shells collide and star formation is disrupted; however, since lower mass stars form first in SNe remnants they can perhaps significantly suppress the formation of more massive stars. At a higher SNa rate, formation of stars more massive than a few solar mass is suppressed; massive stars could still form in the disk after the turbulence generated by shell collisions has subsided and gas has cooled down. This suggests that SNe explosions in a gaseous disk might occur in waves of high and low activity, and during periods of high activity Miller-Scalo IMF is truncated above a few solar mass, and even during periods of lower SNa rate the IMF could be more bottom-heavy than the standard IMF.

### 3.1. The thermal state of the pre-shock gas and the shock-induced stellar IMF

A firm lower limit to the shock front speed, which in turn sets an upper limit to the masses of the stars which may form behind the shock front, is set by the sound speed of the medium upstream of the shock front when SNa shock weakens and turns into a sound wave. In order to calculate the sound speed of the upstream gas, we must determine the thermal state of this gas, and we discuss two possible cases in this subsection.

#### 3.1.1. High supernova rate

For the first case, we consider a galactic disk with a high star formation rate (SFR), in which the dominant process affecting the thermal state of the gas is photo-heating of the gas by massive stars which eventually explode as SNe. Considering that these stars will each live for roughly  $10^7$  yr, the average distance between these massive stars within radius  $r$  of the disk, following equation (18), is

$$d_{sn} \approx 0.6 \frac{r}{\text{1kpc}} f_{sn}(r)^{-1/2} \text{ pc.} \quad (31)$$

The number of ionizing photons emitted per second by such massive stars is  $\gtrsim 10^{49}$  (e.g. Osterbrock & Ferland 2006). Taking the average gas density to be  $\sim 10^3 \text{ cm}^{-3}$ , we find the radius of the Strömgren spheres surrounding massive stars (Strömgren 1939) to be of order  $\sim 1 \text{ pc}$ . Thus, we expect that for an average SNa rates of  $f_{sn} \gtrsim 0.4 \text{ yr}^{-1}$  the H II regions surrounding the massive stars

---

<sup>1</sup>Collision between SNe shells disrupts star formation because of turbulence generated in these collisions. Once turbulence dies out – in about a shock crossing time – star formation can resume provided that the merged shell is not hit again by a high speed shock.

in the disk will overlap, and therefore SNe shocks will propagate into such photoionized regions. Largely independent of the metallicity of the gas, the temperature in such a photoionized region will be of the order of  $10^4$  K, and the sound speed  $\sim 10$  km s $^{-1}$ . Therefore, SNe shocks in this case will generally dissipate and turn into pressure waves once they have slowed to speeds of  $\sim 10$  km s $^{-1}$ . This suggests, following equation (29), that the IMF of stars formed in the material swept up in SNa shocks is likely cut-off at a few solar masses.

### 3.1.2. Low supernova rate

We next consider the case of a lower SFR, corresponding to  $f_{sn} \lesssim 0.4$  yr $^{-1}$ , for which the distance between massive stars is greater than their average Strömngren radii. In this case, SNa shocks will generally propagate into so-called relic H II regions in which gas that was previously photoionized by the progenitor star is recombining and cooling; equations (5) & (6) show that, in general,  $R_s \gtrsim 1$ pc (Strömngren radius) when the SNa shell speed has dropped to  $\sim 10$ km s $^{-1}$ . However, even for larger Strömngren radii, the upstream relic H II region gas can in some cases cool to temperatures well below  $10^4$ K, which allows for the formation of stars with masses greater than a few solar masses.

The results of a numerical calculation of relic H II region gas temperature ahead of the shock are shown in Fig. 1. This calculation assumes that the density of the gas remains constant at the fiducial value of  $n = 10^3$  cm $^{-3}$ , and that the gas cools only radiatively through atomic transitions of metals, which is a reasonable assumption for the case we consider here (but see Jappsen et al. 2009, for the case of star formation in a more isolated environment). In principle, the radiation emitted by the shocked gas can send a radiative precursor ahead of the shock and heat the upstream gas, however, we neglect this effect as at the shock velocities at which the shocks stall, i.e.  $\lesssim 20$  km s $^{-1}$ , radiative precursors do little to ionize or heat the upstream gas (Shull & McKee, 1979).

Figure 1 shows results for four different metallicities:  $10^{-1}$ ,  $10^{-2}$ ,  $10^{-3}$ , and  $10^{-4} Z_{\odot}$ . The metallicity-dependent cooling rate of the gas is taken from Mashchenko et al. (2008), who provide a fitting formula to the cooling function calculated by Bromm et al. (2001). The left panel of Fig. 1 shows the temperature of the upstream gas as a function of the time from the death of the central star. The right panel shows the square of the Mach number for the shock front. The SNa shock will stall once this ratio approaches unity – at this point the shock will turn into a pressure wave.

For metallicities  $\lesssim 10^{-2} Z_{\odot}$  the SNa shock stalls at a time  $t_{stall} \sim 10^5$  yr, when the shock velocity is still  $\sim 10$  km s $^{-1}$ . However, for higher metallicities the shock stalls at later times when  $V_s$  has dropped to a smaller value and thus the maximum mass of SNa-induced stars can become  $M_i \gtrsim 5 M_{\odot}$  for shocks that last for  $\gtrsim 2 \times 10^5$  yr (see eq. 30). We note also that for the case we consider here of  $f_{sn} \lesssim 0.4$ ,  $t_{coll}$  can easily exceed  $t_{stall}$ , and therefore shell collisions will not interfere with SNa-induced formation of these more massive stars at late times.

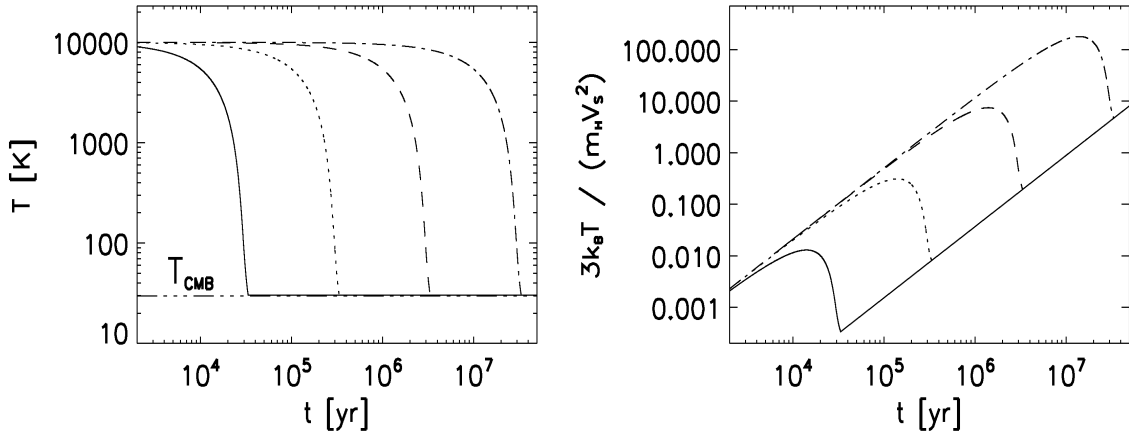


Fig. 1.— The temperature of the medium upstream from the shock front (left panel) and the ratio of the squares of the upstream sound speed and shock front speed during the snowplow phase (right panel), in a cooling relic H II region with gas density of  $10^3 \text{ cm}^{-3}$ . The shock wave turns into a compression wave when the ratio drops to  $\sim 1$ , which occurs at  $t \gtrsim 10^5 \text{ yr}$  for each of the gas metallicities considered here: the curves from left to right correspond to metallicities of  $10^{-1}$ ,  $10^{-2}$ ,  $10^{-3}$ , and  $10^{-4} Z_{\odot}$ , respectively. Note, however, that for lower upstream gas densities this occurs at earlier times, due to the lower cooling rate of the relic H II region gas.

### 3.2. Stars, bulge and black hole

As shown in the last Section, for  $f_{sn} \gtrsim 0.4 \text{ yr}^{-1}$ , stars forming in SNe remnants have peculiar velocities of order  $10\text{--}20 \text{ km s}^{-1}$  in radial direction with respect to the center of the explosion. When viewed from the galactic center the velocities of these newly formed stars in SNe remnants would have a random velocity dispersion of  $\sim 10\text{--}20 \text{ km s}^{-1}$ , and therefore these stars would tend to form a bulge at the center. The velocity dispersion of the newly formed stars would increase with time as these stars are subjected to the stochastic gravitational field of the SNe remnant network. Moreover, these stars will suffer some hydrodynamical drag on their way out of the gaseous disk, and also will be subject to gravitational drag that will modify their velocity dispersion (eg. Artymowicz, 1994; Nayakshin & Cuadra, 2005); the former is likely a small effect due to the small cross-section for star-gas interaction, but the latter can be a significant effect and needs to be included in the calculation to determine the true random velocity distribution of stars formed out of SNe remnants.

The supernova led accretion would also deposit gas in the central parsec region of the galaxy at the rate given by equation (24); at distances smaller than  $\sim 1 \text{ pc}$  the magneto-rotational viscosity (Balbus and Hawley, 1991) is expected to be effective in transporting gas to the black hole at the center. We note that MRI might also operate at larger radius due to heating and ionization produced by SNe.

Let us assume that a fraction  $f_*$  of supernova remnant mass is converted to stars before shells collide with another shell. Using equations (7) and (19) we estimate the star formation rate in SNa remnants to be

$$\dot{M}_* \approx (1.5 \times 10^4 M_\odot) f_* f_{sn}^{0.4} n_3^{0.54} E_{51}^{0.4} r_3^{1.1} \text{ yr}^{-1} \quad (32)$$

Therefore, the ratio of star formation & accretion rates for  $f_{sn} \gtrsim 0.5 \text{ yr}^{-1}$  is  $\sim 5 \times 10^4 f_* f_{sn}^{0.3} n_3^{0.3} E_{51}^{-0.3} r_3^{1.2}$  (eqs. 24 & 32). For  $f_* \sim 10^{-2}$  and  $f_{sn} \sim 1 \text{ yr}^{-1}$  this ratio is of order a few hundred. In the case of low SNa rate (when the remnant survives until its velocity drops to  $\sim 10 \text{ km s}^{-1}$  and then turns into a compression wave) the ratio is  $3 \times 10^4 f_* n_3^{0.7} E_{51}^{-0.7} r_3^2$ , which is also of order a few hundred for  $f_* \sim 10^{-2}$ ; this last expression was obtained by using eqs. 5 & 7 for  $R_s$  &  $M_s$  corresponding to shell velocity of  $10 \text{ km s}^{-1}$  (eq. 6) to calculate star formation and accretion rate (eq. 17).

This ratio of star formation rate to accretion rate is similar to the reported ratio of bulge and BH mass in galaxies (Gebhardt et al. 2000; Ferrarese & Merritt 2000), and the scenario we have described offers a plausible physical explanation for this correlation. We note that a number of well known feed back processes have been left out in the calculations presented in this paper (cf. Cattaneo et al. 2009), and these might significantly modify star formation and accretion rates.

#### 4. Summary

We have analyzed the effect of supernovae occurring within the central kpc region of a gaseous disk on the formation of stars and transport of gas from  $\sim 1 \text{ kpc}$  to a few pc of the galactic center. The outward transport of angular momentum facilitated by SNe explosions allows for the inward transport of gas that feeds the central black hole. This is a process which may take place quite generically in any galactic disk hosting star formation, although it may not be the dominant process affecting black hole accretion.

We have shown that associated with the inward transport of gas swept up by SNe is the shock-induced formation of stars which are born with a random peculiar velocity of  $\sim 10 \text{ km s}^{-1}$ . This velocity dispersion increases with time as a result of the stochastic gravitational field associated with filamentary SNa remnants; The stars formed in SNa remnants contribute to the stellar population of a central bulge.

Due to the divergent velocity field of an expanding SNa shell there is a maximum length scale for fragmentation of shells or an upper limit to the mass of stars formed in SNa remnants; the SNa-induced stellar IMF is cut-off above a few solar masses and more massive stars can only form if and when a SNa shell slows down to  $\sim 10 \text{ km s}^{-1}$ .

We note that numerous observations have suggested connections, such as we have considered in the present work, between star formation, black hole accretion, and the formation of a stellar bulge. Heckman et al. (2004) suggest that star formation and black hole accretion rates are correlated, and Chen et al. (2009) report an empirical relation between supernova rate and gas accretion

rate on the central black hole (see also Xu & Wu 2007). Furthermore, Page et al. (2001) report observations suggesting that central black holes and stellar spheroids form concurrently, and Genzel et al. (2006) describe observations of a galaxy hosting both an accreting black hole and a central stellar bulge, with no evidence of a major merger. Hydrodynamic simulations have demonstrated that SNe feedback may produce spherical distributions of stars in dwarf galaxies (Stinson et al. 2009) and in the inner portions of the Galactic bulge (Nakasato & Nomoto 2003). We would like to point out the recent work of Wang et al. (2009) that models SNe induced turbulence as an effective viscosity and describes the evolution of a gaseous disk.

A limitation of this work is that we have ignored radiative feedback effects which are known to control the steady state accretion rate onto the black hole (e.g. Ostriker et al. 1976, Proga et al 2008, Milosavljevic et al. 2008) and probably also affect the formation rate of stars in the central kpc. Ultimately, large scale simulations resolving the long term evolution of individual SNe remnants, star formation, the multiphase ISM, and the feedback effects of accretion onto a central black hole will be required to more fully elucidate what role SNe-induced accretion and star formation play in galaxy formation.

## 5. Acknowledgments

JLJ gratefully acknowledges the support of a Wendell Gordon Fellowship from the University of Texas at Austin. We thank the referee for many constructive comments that helped improve the presentation significantly.

## REFERENCES

- Artymowicz, P. 1994, *ApJ*, 423, 581
- Balbus, S.A. and Hawley, J.F. 1991, *ApJ*, 376, 214
- Barnes J. E., Hernquist L. E., 1991, *ApJ*, 370, L65
- Barnes, J.E. & Hernquist, L. 1992, *ARA&A*, 30, 705
- Barnes J. E., Hernquist L., 1996, *ApJ*, 471, 115
- Bedogni R., Woodward P. R., 1990, *A&A*, 231, 481
- Blondin, J.M., Wright, E.B., Borkowski, K.J. and Reynolds, S.P. 1998, *ApJ*, 500, 342
- Bratsolis E., Kontizas M., Bellas-Velidis I., 2004, *A&A*, 423, 919
- Bromm, V., Ferrara, A., Coppi, P. S., & Larson, R. B. 2001, *MNRAS*, 328, 969

- Cattaneo, A. et al., 2009, *Nature*, 460, 213
- Chen Y.-M. et al. 2009, *ApJ*, 695, L130
- Chevalier, R.A. 1974, *ApJ*, 188, 501
- Croton D. J., et al., 2006, *MNRAS*, 365, 11
- Di Matteo T., Springel V., Hernquist L., 2005, *Nature*, 433, 604
- Di Matteo T., Colberg J., Springel V., Hernquist L., Sijacki D. 2008, *ApJ*, 676, 33
- Downes, D. & Solomon, P.M. 1998, *ApJ*, 507, 615
- Escala A. 2007, *ApJ*, 671, 1264
- Ferrarese, L. & Merritt, D. 2000, *ApJ*, 539, L9
- Gebhardt, K. et al. 2000, *ApJ*, 539, L13
- Genzel R., et al., 2006, *Nat*, 442, 786
- Granato G. L., De Zotti G., Silva L., Bressan A., Danese L., 2004, *ApJ*, 600, 580
- Heckman T., et al. 2004, *ApJ*, 613, 109
- Hopkins P. F., Hernquist L., Cox, T.J., Di Matteo T., Martini P., Robertson, B., Springel, V., 2005, *ApJ*, 630, 705
- Hopkins P. F., Hernquist L. 2008, *ApJ*, 698, 1550
- Jappsen A.-K., Klessen R. S., Glover S. C. O., MacLow M.-M. 2009, *ApJ*, 696, 1065
- Johnson, J. L., & Bromm, V. 2006, *MNRAS*, 366, 247
- Joung M. K. R., Mac Low, M. M., 2006, *ApJ*, 653, 1266
- Kauffmann G., Haehnelt M., 2000, *MNRAS*, 311, 576
- Kauffmann G., Heckman T. M. 2009, *MNRAS*, 397, 135
- Kawakatu N., Umemura M., 2002, *MNRAS*, 329, 572
- Kormendy, J., Kennicutt, R.C. Jr. 2004, *ARA&A*, 42, 603
- Kroupa, P. 2001, *MNRAS*, 322, 231
- Leão M. R. M., de Gouveia Dal Pino E. M., Faceta-Goncalves D., Melioli C., Geraissate F. G., 2009, *MNRAS*, 394, 157

- Mackey J., Bromm V., Hernquist L., 2003, *ApJ*, 586, 1
- Mashchenko, S., Wadsley, J., & Couchman, H. M. P. 2008, *Science*, 319, 174
- Mihos J. C., Hernquist L., 1996, *ApJ*, 464, 641
- Milosavljevic, M., Couch, S.M., Bromm, V., 2009, *ApJ*, 696, 146
- Nagakura T., Hosokawa T., Omukai K. 2009, *MNRAS*, 399, 2183
- Nakasato N., Nomoto K., 2003, *ApJ*, 588, 842
- Nayakshin, S., Cuadra, J. 2005, *A&A*, 437, 437
- Osterbrock D. E., Ferland G. J. 2006, *Astrophysics of Gaseous Nebulae and Active Galactic Nuclei*, University Science, Sausalito
- Ostriker, J., Weaver, R., Yahil, A., McCray, R., 1976, *ApJ*, 208, L61
- Page M. J., Stevens J. A., Mittaz J. P. D., Carrera F. J., 2001, *Sci*, 294, 2516
- Proga, D., Ostriker, J., Kurosawa, R., 2008, *ApJ*, 676, 101
- Ryu, D. & Goodman, J. 1992, *ApJ*, 388, 438
- Sakuma M., Susa H., 2009, *ApJ*, 698, 155
- Sanders, D.B. & Mirabel, I.F. 1996, *ARA&A*, 34, 749
- Sanders D. B., Soifer B. T., Elias J. H., Madore B. F., Matthews K., Neugebauer G., Scoville N. Z., 1988, *ApJ*, 325, 74
- Scalo, J.M. 1986, *Fundamentals of Cosmic Physics*, vol. 11, p 1-278
- Shull J. M., McKee C. F., 1979, *ApJ*, 227, 131
- Springel V., Di Matteo T., Hernquist L., 2005, *MNRAS*, 361, 776
- Stacy A. & Bromm V. 2010, *MNRAS*, accepted (arXiv:0908.0712)
- Stinson G. S., et al. 2009, *MNRAS*, 395, 1455
- Strömgren B. 1939, *ApJ*, 89, 526
- Wada, K & Norman, C.A. 2001, *ApJ*, 547, 172
- Wang J.-M., et al., 2009, *ApJ*, 701, 7
- Woodward P. R. 1976 *ApJ*, 207, 484

Xu B. X., Wu X. B. 2007, ApJ, 667, 92

Xu B. X., Wu X. B., 2007, ApJ, 667, 92

Yamada M., Nishi R., 1998, ApJ, 505, 148